Feasibility study of high-rate dissolved air flotation process for rapid wastewater treatment

Mi-Sug Kim, Seok Dockko, Gyunnam Myung and Dong-Heui Kwak

ABSTRACT

One advantage of the flotation system is its high applicability as a compact facility. Recently, research for the introduction of additional high-rate dissolved air flotation (DAF) into conventional water treatment plants has been progressing in areas of remodeling water treatment plants, advanced treatment, and combined sewer overflow (CSO) treatment. For successful design and operation of high-rate DAF, laboratory experiments to verify model results and estimate standard values of major parameters by model simulation were performed in this study. With the model simulation having a population balance concept, an operational analysis of bubble-floc aggregates considering a hydraulic situation in the separation zone during high-rate DAF was conducted. Based on the model simulation results, a basic level for high-rate DAF design at a hydraulic loading rate of 30 m/h was determined. On the basis of population balance theory, it can describe the process of bubble-floc aggregate formation at a contact zone and calculate the rate of transfer into the separation zone.

Key words | dissolved air flotation, high rate, microbubble, particle separation, population balance

Mi-Sug Kim
Environment and Health Science,
Jeonju University,
303 Cheonjam-ro Wansan-gu,
Jeonju, Jeonbuk, 560-759,
Republic of Korea

Seok Dockko
Department of Civil and Environmental Engineering,
Dankook University,
119 Dandae-ro Dongnam-gu,
Cheoan, Chungnam, 330-714,
Republic of Korea

Gyunnam Myung
Newentec Energy & Environment, Inc.,
224-5 Kwanyang-dong Dongan-gu,
Anyang, Kyeongki, 431-060,
Republic of Korea

Dong-Heui Kwak (corresponding author)
Department of Environmental and Chemical Engineering,
Seonam University,
439 Chunhyang-ro, Namwon, 590-711, Jeonbuk,
Republic of Korea
E-mail: *kwak124@hanmail.net*

INTRODUCTION

The key technology of high-rate dissolved air flotation (DAF) is achieved by rapid separation of bubble-floc aggregates. According to the specific gravity of the floc in the separation zone, bubble-floc aggregates have a slower rise velocity than microbubbles. Considering the rise velocity of the aggregates, the downward flow rate in the separation zone of the flotation tank dominates the overall efficiency of the DAF process (Edzwald *et al.* 1999). When designing the high rate DAF, much attention is required because the hydraulic loading rate is faster than the rise velocity of the bubbles. As such, it is highly possible that the treated water is discharged before bubbles and flocs are attached or before the aggregates rise to the water surface. The ideal direction pattern that is maintained in the internal portion of the tank has been suggested as the point that prevents this phenomenon.

The flotation tank consists of a contact zone and separation zone, and the excellence of DAF performance is apparent when the three features of the ideal flow pattern in the separation zone are formed. The three features of the ideal flow pattern include the stratified flow of the surface, the vertical plug flow below the stratified flow, and the horizontal plug flow at the bottom floor. However, this ideal theory for the conventional DAF process with hydraulic load rate (5–15 m/h) does not work in the high-rate DAF process (30 m/h) because the hydraulic load (hydraulic loadings) rate exceeds the rise velocity (Edzwald 2010). The high-speed system can remove free bubbles and the bubble-floc aggregates in the stratified flow area of the separation zone. In particular, research on the hydraulic flow characteristics and stratified flow that occur in the separation zone is required in order to merge the flow pattern in the model. The flow pattern through the separation zone does not follow the simple ideal case of plug flow in the vertical direction. It is influenced by the velocity of

doi: 10.2166/aqua.2015.025

water above the baffle (cross-flow velocity), the hydraulic loading, the aspect ratio (length to width ratio), how water is withdrawn at the outlet, and the air bubble suspension in the upper part of the separation zone (Lundh *et al.* 2002).

The basic research carried out over the last 30 years has laid the groundwork for the development of high-rate DAF technology (Wang *et al.* 2005). According to previous studies (Haarhoff & Edzwald 2001; Rubio *et al.* 2007; Oliveira & Rubio 2012), the major trend is to decrease flocculation times, increase DAF loadings, and develop compact (small 'footprint' areas) and efficient treatment units. Small aggregates can be easily removed at high DAF (modern design) rates, contradicting the conventional bias that large floc units and bubbles are required for successful separation. In other words, the effective separation of the combined bubble-floc aggregates with small bubbles is determined by the flow rate in the separation zone of the DAF process. While larger separation zones lead to higher separation efficiency of the bubble-floc aggregates, they also create an inefficient situation by increasing the process size. Therefore, technology for the maximum separation of the bubble-floc aggregates through high separation speed in the separation zone while maintaining a minimal physical size is important. Lakghomi *et al.* (2012) reported that increasing the amount of air improved the removal efficiency and generated a useful stratified horizontal flow pattern.

Because many previous studies report a threshold for high-rate DAF with a hydraulic load rate over 0.4167 m/min (or 25 m/h), modeling and experimental studies are required for water treatment through various methods of flotation separation and measuring the rise velocity of the bubble-floc aggregates for the proper operation and design of high-rate DAF. Thus, the purpose of this study is to understand the characteristics of operating and designing parameters for the DAF process and to evaluate the scope and applicability of the proposed threshold for high-rate DAF with a hydraulic load rate of 0.5 m/min (or 30 m/h) for treating combined sewer overflows (CSOs). In order to successfully design and operate high-rate DAF, standard values of major parameters were determined through model simulation, and laboratory tests were performed to verify the estimated model values in this study. Considering the hydraulic situation in the separation zone and the operational analysis of the bubble-floc aggregates, a basic level of high-rate DAF with a hydraulic loading rate of 30 m/h for design has been determined by simulating the model introducing the population balance concept. The model simulation can describe the formation process of bubble-floc aggregates in the contact zone and calculate the transfer rate of the formed aggregates that transfer into the separation zone. Focusing on the change of the bubble volume fraction in the separation zone, depending upon the hydraulic loading rate, the model simulation was conducted using the population balance turbulence (PBT) model. Laboratory tests were conducted to measure the rise velocity of the bubbles and the bubble-floc aggregates as a function of the run-time change and the depth change of the milky water layer.

MATERIALS AND METHODS

Theoretical approach

The population balance for describing the process of bubble-floc collision and attachment was formulated by counting the number of flocs attached (i-bubbles n_i at mixing time t). On the basis of the assumptions reported by Fukushi *et al.* (1995) and modified by Leppinen *et al.* (2001), the number of flocs attached, i-bubbles n_i, is represented by ordinary differential equations as follows:

$$\frac{dn_0}{dt} = -k\alpha_0 n_0 n_{\text{bubbles}} \tag{1}$$

$$\frac{dn_i}{dt} = -(k\alpha_i n_i n_{\text{bubbles}} - k\alpha_{i-1} n_{i-1} n_{\text{bubbles}}) \quad \text{when} \quad i = 1 \text{ to } i_{\max}. \tag{2}$$

where k is the turbulent collision rate constant, $n_{bubbles}$ is the number of bubbles per unit volume, and α_i is the adhesion efficiency.

In order to calculate the rise velocity of bubbles, flocs, and bubble-floc aggregates, the flotation principle according to Stokes' law can be applied. The governing equation in air flotation separation, as in all gravity controlled processes, is Stokes' law (at least in laminar flow), which is used to

compute the rise rate of bubbles, flocs, and agglomerates (V_b, V_f, and V_{fb}). Considering the bubble rise velocity, V_b, for a water column under no-loading condition with stagnating water flow, Stokes' law describes the rise velocity of bubbles, V_b, for Reynolds number, $Re \leq 1$, of bubble diameter $d_b \leq 125\,\mu m$ at 20 °C according to Equation (3):

$$V_b = \frac{g(\rho_w - \rho_b)d_b^2}{18\mu_w} \tag{3}$$

where V_b is the terminal rise velocity of the bubbles, cm/s; g is the gravitational constant, 980 cm/s^2; d_b is the effective diameter of the bubbles, cm; ρ_b is the density of the bubbles, g/cm^3; ρ_w is the density of the aqueous phase, g/cm^3; and μ_w is the viscosity of the aqueous phase, *cp*.

If a balance between the bubble rise velocity by buoyancy and the bubble falling velocity by downward water flow occurs in the separation zone, the bubble diameter and the rise velocity are estimated at 120 μm and 24.8 m/h, respectively. It is difficult to maintain a steady flow condition because the 24.8 m/h of the maximum bubble rise velocity is slower than the 30 m/h of the hydraulic loading rate in this study. When increasing the bubble rise velocity by expanding the bubble diameter, the laminar flow does not appear in the bubble layer formation (Ryu *et al.* 2011). Therefore, it is necessary to compare the bubble layer formed by the 120 μm bubbles with the results in the time domain forming the stratified flow according to the bubble layer. Haarhoff & Edzwald (2004) proposed the theoretical rise velocity of the bubble-floc aggregates for $Re \leq 1$ as shown in Equation (4). If Re is in the transition region, $1 < Re < 50$, Equation (5) can be used to calculate the rise velocity. For solving Equation (5), it is required to first calculate Equation (6) for the diameter of the aggregates, and Equation (7) for the density of the aggregates, to be dependent on the attached bubble number:

$$V_{fb} = 4g(\rho_w - \rho_{fb})\frac{d_{fb}^2}{3K\mu_w} \quad \text{for} \quad \mathrm{Re} \leq 1,\ d_{fb} < 160\,\mu m \tag{4}$$

$$V_{fb} = \left(\frac{4}{3K}\right)^{0.8}(g^{0.8}(\rho_w - \rho_{fb})^{0.8}d_{fb}^{1.4}/(\rho_w)^{0.2}(\mu_w)^{0.6}) \quad \text{for} \quad 1 < \mathrm{Re} < 50 \tag{5}$$

$$d_{fb} = (d_f^3 + N_b d_b^3)^{\frac{1}{3}} \tag{6}$$

$$\rho_{fb} = \rho_f d_f^3 + N_b \rho_b \frac{d_b^3}{d_f^3} + N_b d_b^3 \tag{7}$$

where V_{fb} is the terminal rise velocity of the agglomerate, cm/s; ρ_{fb} is the density of the agglomerate, g/cm^3; ρ_w is the density of the aqueous phase, g/cm^3; μ_w is the viscosity of the aqueous phase, *cp*; and N_b is the number of bubbles per unit volume.

K in Equation (8) is described in the form of agglomerates, and the effects of K will be described for the resistance increase in drag. When large bubbles that are greater than 100 μm are attached on a small floc of 40 μm, the aggregates are substantially spherical and K is 24. If the floc is significantly larger than 100 μm, the aggregates approach the form of floc and K is 45. Since K is 24 of the floc in 40 μm, and K is 45 of the floc in 170 μm, it is assumed that K becomes gradually smaller:

$$K = \frac{16N_b + 45\left(\frac{d_f}{d_b}\right)^2}{\left(N_b + \left(\frac{d_f}{d_b}\right)^2\right)} \tag{8}$$

Tambo *et al.* (1986) formulized Equation (9) to calculate the maximum number of bubbles attached on the floc:

$$\mathrm{N}_{b,\max} = \pi\left(\frac{d_f}{d_b}\right)^2 \tag{9}$$

Many aggregates formed in the contact zone rise to the top layer. However, a portion of them is moved into the separation zone and rises into the top layer to be separated if the rise velocity in the laminar state is greater than the hydraulic loading rate. Design and performance of the footprint area for removal of free bubbles and of the bubble-floc aggregates applying the Hazen theory of the sedimentation tank have been considered the idealized DAF tank. The vertical plug flow is assumed to occur over the main part of the separation zone (i.e., the clarification section). The horizontal flow

below the bubble-floc aggregate layer and above the baffle for separating the contact zone and the separation zone is ignored when evaluating the clarification performance. The free bubbles and the bubble-floc aggregates are removed if the rise velocities, V_b and V_{fb}, exceed the hydraulic loading rate (V_{sz-hl}) in the separation zone. As mentioned above, the standard value of rise velocity of the bubbles and the bubble-floc aggregates is approximately 20 m/h. Therefore, these bubbles and the aggregates are removed when the hydraulic loading rate is less than 20 m/h in the separation zone. Edzwald (2010) summarizes that the hydraulic loading rate is conservative enough in order to evaluate the performance of the conventional DAF system. The typical hydraulic loading rate of the conventional DAF system is 5–15 m/h. When considering the footprint area (A_{sz}) of only the separation zone and having a recycle rate of 10%, the hydraulic loading rate in the separation zone is still 20 m/h or less. Thus, even though the plug flow does not occur, the hydraulic loading rate is used to design the separation zone of the conventional DAF system.

For the high-rate DAF system in which the hydraulic loading rate exceeds the rise velocity of the bubbles and the aggregates, the separation zone must consider the flow path or pattern because it is inadequate when modeling the separation zone under the simple and ideal condition. The hydraulic loading rate V_{sz-hl} acting on the separation zone is as follows:

$$V_{fb} \geq V_{sz-hl} = \frac{Q}{A_{sz}} \tag{10}$$

If considering the recycle ratio:

$$V_{fb} \geq V_{sz-hl} = \frac{(Q+Q_r)}{A_{sz}} \tag{11}$$

If considering the dead space m, which exists in the real separation zone:

$$V_{fb} \geq \frac{(Q+Q_r)H_{sz}}{A_{sz}H_{sz}(1-m)} = \frac{(Q+Q_r)}{A_{sz}(1-m)} = \frac{V_{sz-hl}}{(1-m)}. \tag{12}$$

The rise velocity of the aggregates reaches the maximum when the occurrence of such dead space is suppressed (Behin & Bahrami 2012). The separation area can be calculated according to changing the recycle flow rate as functions of the varying recycle ratio R and the fixed hydraulic loading rate of 30 m/h (0.5 m/min). In addition, the rise velocity V_{fb} of the aggregates may be used to calculate the hydraulic loading rate V_{sz-hl} and the dead space m.

For theoretical experiments, the PBT model written by MATLAB software was used for simulation of size distribution, rising velocity, time, and removal efficiency of bubbles, flocs, and floc-bubble aggregates. The simulation was performed using the following information: floc sizes between 0.1 and 210 μm, bubble size of 100 μm, initial density of flocs 1,100 kg/m^3 and 500 kg/m^3 (Santana *et al.* 2012), and hydraulic loading rate V_{sz-hl} of 0.5 m/min (or 30 m/h) in order to examine the change in the rise velocity of one aggregate formed by one bubble attached on one floc; the initial number concentration of flocs, N_{p0}, 2,000, the number of bubbles N_{bi} from 10^5 bubbles to 10^6 for estimating the removal efficiency of bubble-floc aggregates; inflow rate of 1.62 m^3/h and recycle rate of 10%, bubble diameter d_b of 120 μm, floc diameter d_f of 250 μm, and an initial density of 900 kg/m^3 in order to investigate critical values of parameters.

Labs Test

The Labs Test was performed in order to measure the rise velocity of the bubbles and the bubble-floc aggregates. The experimental apparatus in the Labs Test was assembled by connecting a batch reactor, as shown in Figure 1. The rise velocity was measured by examining the change in the bubble layer (milky water layer) after injecting the saturated water into the water column in the batch reactor once, as opposed to examining the continuous flow. The experiments were conducted in the batch reactor, which was not divided into a contact zone and separation zone. The rise velocities of the microbubbles and the aggregates were measured by measuring the run-time change and the depth change of the milky water layer (i.e., the bubble cloud or bubble layer) after turbulent mixing with injection of the dissolved air bubbles contacting the flocs formed in the sample of the batch reactor. The flotation reactor of 1.5 L capacity (7 cm diameter and 50 cm height) used in the experiment was made with transparent acrylic. The microbubbles were supplied into the flotation reactor as dissolving air under

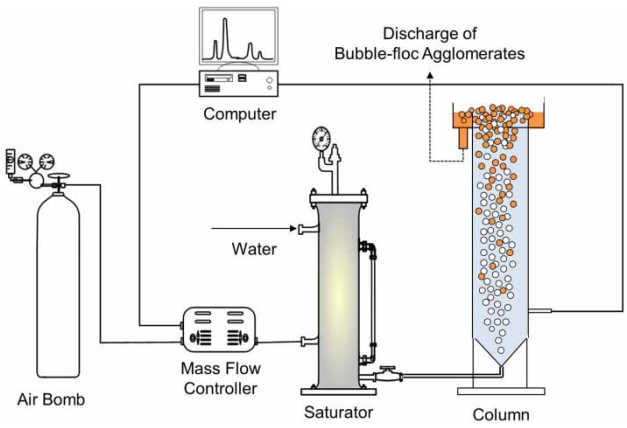

Figure 1 | Schematic diagram of lab-scale pilot plant used in this study.

the pressure range of 4.0 ± 0.1 atm in the stainless steel saturator.

The Labs Test for rise velocity verification of bubble and bubble-floc aggregates was performed in order to measure the rise velocity of the bubbles and the bubble-floc aggregates. In the experiments, two types of flocs were used: the coagulation floc and the flocculation floc. The coagulation floc (Floc Type 1) was formed by rapid mixing at 60 revolutions per minute (rpm) for 30 s, while the flocculation floc (Floc Type 2) was prepared by slow mixing at 30 rpm for 2 min in order to make the floc larger than after the rapid mixing.

RESULTS AND DISCUSSION

Rise velocity of bubble and bubble-floc aggregates

According to the hydraulic loading rate increase, the mean velocity of the separation tank is increased and the microbubbles may move to the deep portion of the separation tank. These microbubbles determine the rise velocity as a function of the bubble volume. While many aggregates are separated by rising to the top layer, a portion of them are separated by rising to the top layer when their rise velocities are greater than the hydraulic loading rate in the laminar flow state after moving to the separation zone. If the microbubbles move into the separation zone and do not increase in size, the rise rate is low. However, the bubbles in the separation zone are bigger than those in the contact zone (Haarhoff & Edzwald 2004). The bubbles that are released from the nozzle are distributed at a size of $40 \sim 60$ μm in the contact zone, but they are distributed at a size of 50–150 μm in the separation zone through growth, coalescence, and clustering phenomena (Leppinen & Dalziel 2004).

This study checked the conditions for rising into the upper bubble layer, combining free bubbles, and the part of the aggregate that is moved into the separation zone. As shown in Figure 2, laboratory experiments were performed to examine the various bubble size changes as a function of pressure. Figure 2 shows that the bubbles in the upper bubble layer are much larger than the bubbles in the bottom of the bubble layer. Figure 3 presented the Reynolds number (Re) and the rise velocity of the microbubbles. The rise velocity of the bubbles smaller than 150 μm is 0.83 cm/s (0.5 m/min or 30 m/h) for $Re < 1$.

In order to examine the change in the rise velocity of one aggregate formed by one bubble attached on one floc, a simulation was performed using the following information: floc sizes between 0.1 and 210 μm, bubble size of 100 μm, and initial density of flocs 1,100 and 500 kg/m^3 (Santana *et al.* 2012). The simulation results are shown in Figure 4 compared with the hydraulic loading rate V_{sz-hl} of 0.5 m/min (or 30 m/h). Figure 4 indicates the rise velocity of the aggregates for one bubble of 100 μm attached on the various floc sizes with an initial density of 1,100 and

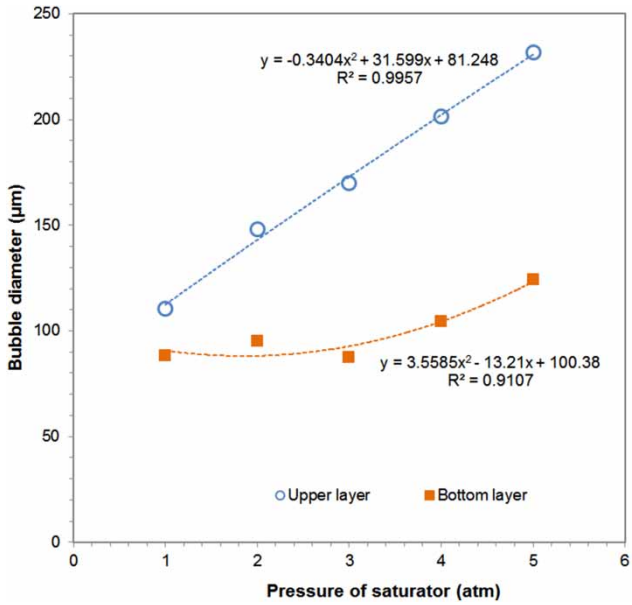

Figure 2 | Bubble diameter change due to pressure formed in upper layer and bottom layer of the flotation cell.

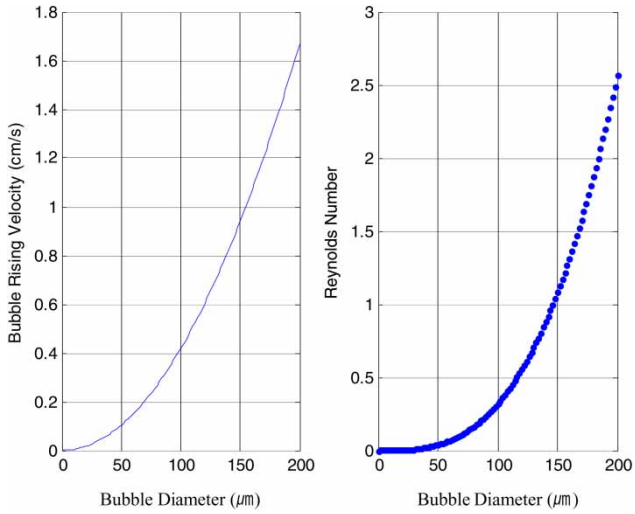

Figure 3 | Rise velocity of bubble and Reynolds number depending on bubble sizes.

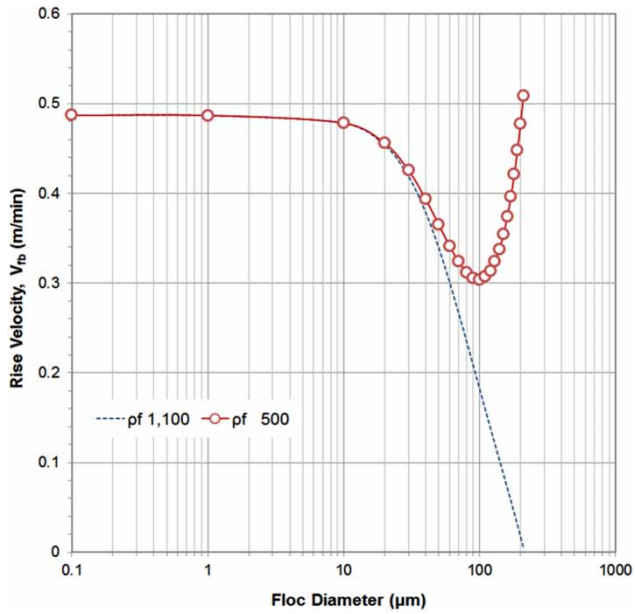

Figure 4 | Bubble-floc aggregate rise velocity depending on floc size for two initial floc densities 500 kg/m^3 and 1,100 kg/m^3.

500 kg/m^3. For flocs that are 10 μm or less, the rise velocity of the aggregates is approximately 0.33 m/min (or 20 m/h), and it is the same with the rise velocity for the same size bubbles only. In the case of an initial floc density of 1,100 kg/m^3 and a floc of 200 μm, the rise velocity of the aggregates approached zero. In the case of an initial floc density of 500 kg/m^3, the rise velocity of the aggregates increased when one bubble was attached on the floc size of 100 μm or more, and it was over 0.5 m/min (or 30 m/h) when the floc size was 210 μm.

Rise velocity of bubble-floc aggregates in terms of bubble size and number

While the rise velocity of the large floc achieved a high rate, the attachment of many bubbles was required. The rise velocity V_{fbi} was defined as the proper rise velocity of the proper bubble-floc aggregates when the rise velocity V_{fbi} became greater than the hydraulic loading rate V_{sz-hl} of 0.5 m/min (or 30 m/h) and the rise time t_r was faster than the retention time τ_s. In order to check the effect of the number of bubbles attached on the floc, the rise velocity of the aggregates was calculated according to the bubble number attached on a 210 μm floc having an initial floc density of 500 kg/m^3. The calculated rise velocity is summarized in Table 1. When one bubble is attached on one floc, N_{b1} is defined as the number of bubbles, V_{fb1} is indicated as the rise velocity when $V_{fb1} \geq V_{sz-hl}$, and $t_r \leq \tau_s$ for meeting flotation condition in the separation zone. Therefore, in the case of a bubble diameter of 100 μm, even though the rise velocity is faster than the hydraulic loading rate, two bubbles are needed to produce a rise time faster than the retention time, as shown in Table 2. When the rise velocity V_{fbi} is faster than the hydraulic loading rate V_{sz-hl}

Table 1 | Information for bubbles attached on the 210 μm floc and bubble-floc aggregate rise velocity

Bubble diameter (μm)	10	20	30	40	50	60	70	80	90	100
N_{bmax}	1,385	346	154	87	55	38	28	22	17	14
N_{b1}	1	1	1	1	1	1	1	1	1	1
V_{fb1} m/min	0.38	0.38	0.39	0.39	0.40	0.42	0.43	0.45	0.48	0.51
N_{bi}	398	83	32	16	10	6	4	3	3	2
V_{fbi} m/min	0.59	0.59	0.59	0.59	0.61	0.59	0.59	0.60	0.68	0.64
V_{sz-hl} m/min	0.5	0.5	0.5	0.5	0.5	0.5	0.5	0.5	0.5	0.5

Table 2 | Dead space and rise time for high-rate DAF

Bubble diameter (μm)	Attached bubbles (number)	Rise velocity, V_{fb} (m/min)	Reynolds number, *Re* (number)	Dead space, m (number)	Rise time, t_r (min)
10	398	0.588	2.08	0.0003	0.397276
20	83	0.589	2.10	0.0020	0.396595
30	32	0.590	2.12	0.0022	0.396502
40	16	0.589	2.13	0.0020	0.396594
50	10	0.606	2.20	0.0289	0.385897
60	6	0.593	2.16	0.0083	0.394101
70	4	0.589	2.15	0.0016	0.396761
80	3	0.600	2.20	0.0197	0.389543
90	3	0.679	2.54	0.1335	0.34432
100	2	0.641	2.38	0.0819	0.364826

and the rise time t_r is faster than the retention time τ_s, N_{bi} is defined as the proper number of bubbles in order to form the bubble-floc aggregates.

The maximum number of bubbles attached on the 210 μm floc is 1,385 for the 10 μm bubbles and 14 for 100 μm bubbles, that is, the smaller bubbles lead to more bubble attachments (Han 2002). In order to examine the rise velocity of the aggregates according to the attached number of bubbles, the rise velocity when only one bubble is attached needs to be calculated. When the calculated rise velocity was compared with the hydraulic loading rate, the rise velocity of the aggregates attached by a bubble of only 100 μm was greater than the hydraulic loading rate of 0.5 m/min (30 m/h). However, it did not meet the flotation condition in the separation zone. The flotation condition in the separation zone is met when the rise velocity of the aggregates is greater than the hydraulic loading rate (i.e., $V_{fb} \geq V_{sz-hl}$) and the rise time t_r is faster than the retention time τ_s. To reach $t_r \leq \tau_s$, the attached number of bubbles, N_{bi}, was 398 bubbles for the bubble size 10 μm and two bubbles for the bubble size 100 μm. Ranging between 0.59 and 0.68 m/min, the calculated rise velocity of the aggregates was faster than the hydraulic loading rate of 0.5 m/min (or 30 m/h), but the Reynolds number *Re* was in the transition region between 1 and 50.

As shown in Table 1, the rise velocity changed according to the size of bubbles. As an increase in the hydraulic loading rate V_{sz-hl} of 0.5 m/min (or 30 m/h) indicates an increase of inflow rate, the recycling flow rate was increased if the recycle ratio was fixed. If the flow rate of the circulating water is not increased, the density of the bubble layer in the separating tank is reduced, and the quality of the treated water worsens. If the flow rate in the contact zone is too rapid, the possibility of collision between bubble and floc becomes smaller and the contact zone will not be sufficiently used.

Removal efficiency of bubble-floc aggregates in terms of attached bubble number on a floc

Figure 5 shows the removal efficiency X when the bubbles injected into the contact zone collide and attach on a floc during the contact time. The floc is flocculated particles which form floc-bubble aggregates when they meet with bubbles in the contact zone during the contact time. The initial number of the concentration of flocs, N_{p0}, is 2,000 in this study. By colliding and attaching during the contact time, most of the formed aggregates were removed by floating to the top bubble layer as fast as the removal efficiency X. Free bubbles and flocs that did not collide/attach and the remainder of the formed aggregates with a rise velocity slower than the hydraulic loading rate would be removed by increasing the rise velocity and causing the attachment of free bubbles in the separation zone or their release according to the water flow. By increasing the number of bubbles from 10^5 bubbles to 10^6, the removal efficiency X approached near 100% within the first few seconds, as shown in Figure 5. If the removal efficiency X increases, it is considered to increase the separation efficiency of the

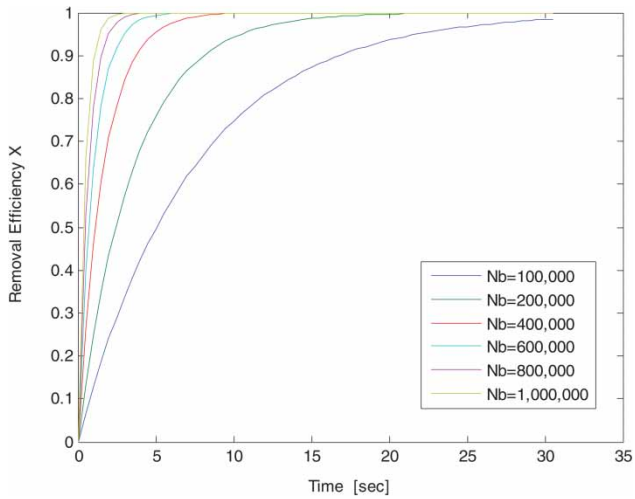

Figure 5 | Removal efficiency of bubble-floc aggregates depending on the bubble number calculated by the PBT model.

untreated flocs and aggregates in the separation zone of the high-rate DAF.

The rise velocity of the aggregates as a function of the recycle ratio was examined in order to check the degree of dead space to be considered when designing the separation tank. Considering several parameters, including a hydraulic loading rate of 30 m/h, an inflow rate of 1.62 m^3/h, and a recycle rate of 10%, the results of the retention time, the rise time, the rise velocity of the aggregates, the Reynolds number, and the dead space are summarized in Table 2.

When considering the bubble diameter d_b of 120 μm and the floc diameter d_f of 250 μm, and having an initial density of 900 kg/m^3, Figure 6 presents the results of several parameters including aggregate diameter (D_{fb}), critical floc diameter (*Critical* D_f), and critical aggregate diameter (*Critical* D_{fb}). The aggregate diameter D_{fb} increased as the number of bubbles attached increased; it increased from 125 μm when one bubble attached to 160 μm when ten bubbles attached, and the critical aggregate diameter, *Critical* D_{fb}, decreased from 60 to 20 μm by increasing the number of bubbles attached. If the critical aggregate diameter is smaller than the diameters of the microbubbles, flocs, and aggregates, the fate of the aggregates in the separation zone was influenced by the difference between the drag force due to the surrounding stream flow and the buoyancy due to the bubble volume. The smaller microbubbles, especially those with diameters less than 10 μm, were discharged easily with low flow velocity.

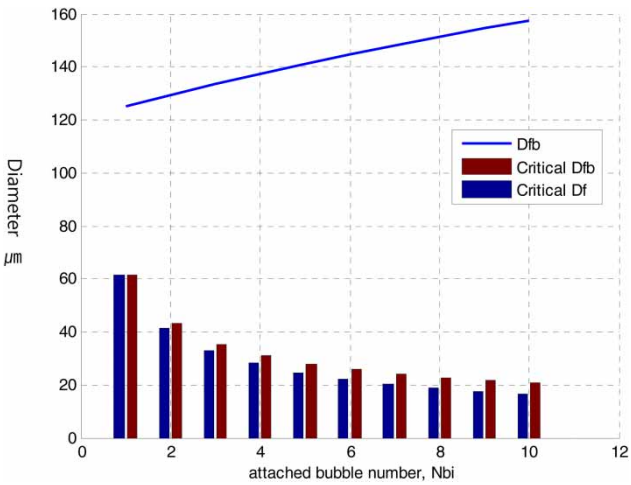

Figure 6 | Critical bubble-floc aggregate diameter, *Critical* D_{fb}, and critical floc diameter, *Critical* D_f, related to attached bubble numbers (initial floc diameter = 250 μm, bubble diameter = 120 μm, ρf 900 < ρw 1,000, D_{fb} = diameter of bubble-floc aggregate).

Labs Test for rise velocity verification of bubble and bubble-floc aggregates

The Labs Test was performed in order to measure the rise velocity of the bubbles and the bubble-floc aggregates. As performed in the previous study of Kwak & Kim (2013), Figure 7 shows the bubble diameter distribution and the entire accumulated bubble volume. The bubbles were mostly distributed in the range of 30 to 60 μm. The bubbles with diameters of 70 μm or less were approximately 95% of the total and the entire accumulated bubble volume was 0.0005351 cm^3.

Figure 8 presents the measurement results of the rise velocities of the bubbles and bubble-floc aggregates based on the bubble capacity of the bubble layer that was collected at the top of the 0.4 m-height water column of the 0.5 m-height flotation column. The bubble cloud layer was formed by turbulent mixing when the dissolved bubbles were injected into the water column. The depth of the bubble cloud layer was made thinner by the rising bubbles and aggregates from the bottom of the reactor with time change. As shown in Figure 8, the change in the bubble cloud layer is indicated as a function of the fraction of the bubble cloud depth. Then, the rise velocities of the bubbles and aggregates were changed by the change in the bubble cloud layer. That is, the initial fraction of the bubble cloud depth was 1, and the rise velocity was at its maximum when the fraction of the bubble cloud depth was 1. When the fraction of the bubble cloud depth was getting smaller, the rise velocity decreased and tended to change differently between the bubbles and the aggregates. The rise velocity of bubbles rapidly decreased to roughly 70 m/h from 700 m/h until the fraction of the bubble cloud depth decreased from 1 to 0.75. In the middle fraction of 0.75 to 0.1, the bubble rise velocity tended to decrease very smoothly to 30 m/h from 70 m/h. In the low fraction between 0.1 and 0.01, the rise velocity of the bubbles was approximately 15 m/h, being reduced by half. The rise velocities of two aggregate types formed by Floc Type 1 and Floc Type 2 were measured. There was little difference between the two types of aggregates. However, the results showed that the rise velocities between them tended to change opposite to each other for a rise velocity of 0.5 m/min (or 30 m/h) at the bubble cloud depth fraction of approximately 0.35. Furthermore, the rise velocities of the bubbles and aggregates were

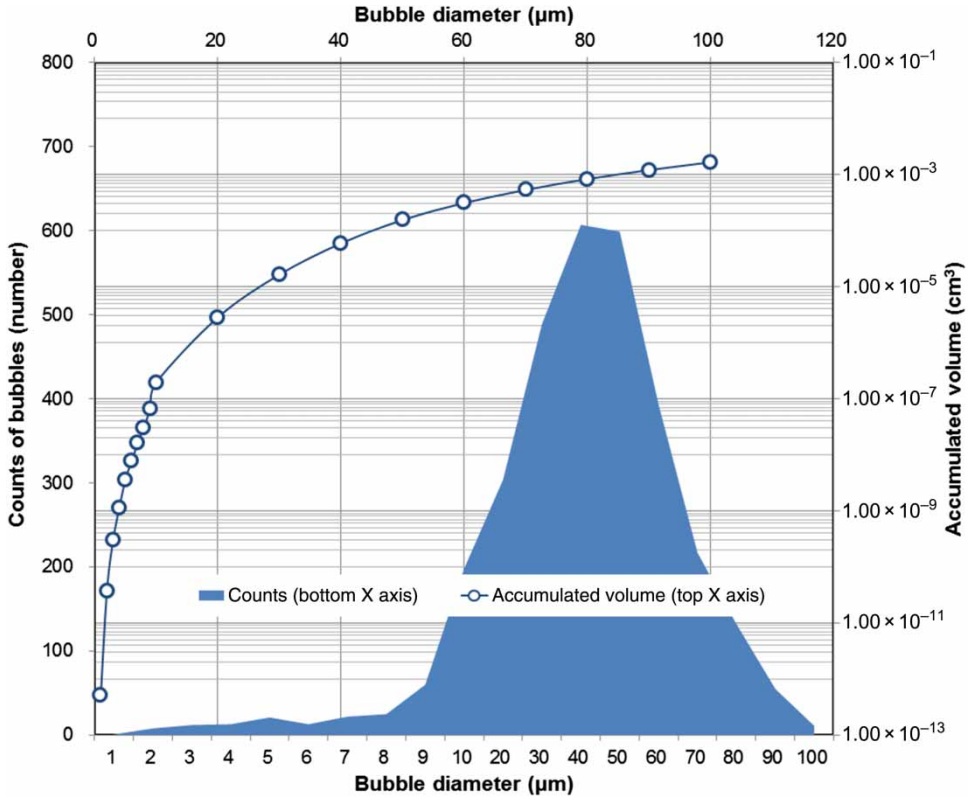

Figure 7 | Bubble size distribution in terms of diameter of bubbles.

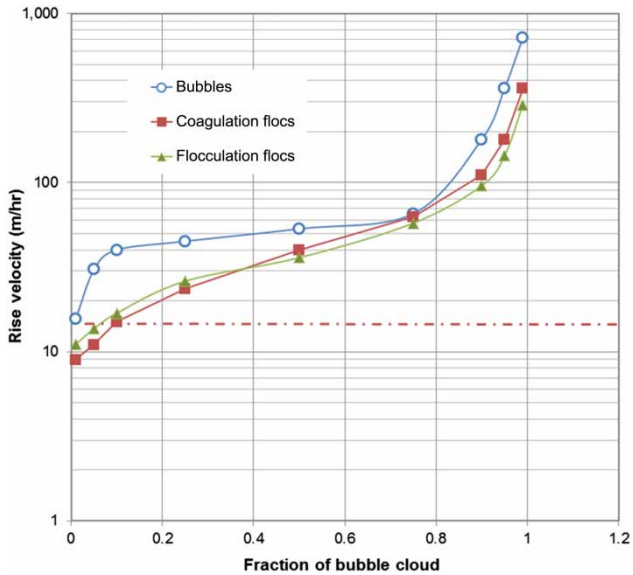

Figure 8 | Rise velocity of bubbles and bubble-floc aggregates with change of bubble cloud bed depth.

similar; approximately 70 m/h at 0.75 fraction of the bubble cloud depth. According to the experiments of this study, the rise velocity of the bubbles and aggregates was over 0.5 m/min (or 30 m/h) when the fraction of the bubble cloud depth was higher than 0.35.

CONCLUSIONS

For flotation in the separation zone during laminar flow, problems arise with a hydraulic loading rate over 0.4167 m/min (25 m/h) because it causes turbulent flow. Thus, a change in the design of the flotation tank is required. When the hydraulic loading rate in the separation zone is 0.4167 m/min to 0.667 m/min (25 to 40 m/h), obtaining sufficient flotation space or maintaining a thicker microbubble cloud layer is required in the separation zone; that is, a thicker bubble layer leads to a higher removal efficiency. The bubble layer can be made much thicker to raise capacity when using the high-rate DAF. In this study, a simulation using a population balance in turbulence (PBT) model concept was conducted and simulation results were verified through laboratory experiments. The change in bubble volume fraction in the high-rate

DAF tank using a hydraulic loading rate of 30 m/h was examined through simulation and laboratory experiments.

For the high-rate DAF processes such as CSO treatment, using a hydraulic load rate of 30 m/h to be feasible, these conditions must be satisfied: (1) the flow pattern in the separation zone and stratified flow must be maintained and (2) when dispersion of flocs is very rare, the probability of contact between flocs and bubbles is increased, as many bubbles are supplied. Therefore, the rise velocity of the aggregates is increased when these conditions are satisfied. Especially, the following two things must be considered carefully: (1) if the bubble diameter is less, the collision efficiency between the floc and bubble is increased but the rise velocity of the bubble-floc aggregate becomes slow; and (2) along the flow of the effluent, bubble-floc aggregates smaller than the critical bubble-floc aggregate are discharged with flocs that are not combined with bubbles.

In this study, the effect of the bubble volume fraction in the separation zone of the high-rate DAF on hydraulic loading rate was confirmed. In addition, the hydraulic loading rate may influence the change of flow. The change of flow in the high-rate DAF tank as a function of the hydraulic loading rate may change the tendency of rise along the sloped baffle after inflow water is mixed with recycled water. Computational fluid dynamics (CFD) performance is required to estimate a more accurate change of flow. Therefore, future studies may focus on CFD simulation using information obtained from the results of the current study.

ACKNOWLEDGEMENTS

This study is supported by the Korea Ministry of Environment (MOE) as 'Eco-Innovation (EI) Program' (E314-00015-0412-1) and the National Research Foundation of Korea (NRF) with grants from the Ministry of Education in Korea, 2014 (NRF-2012R1A1A4A01010342).

REFERENCES

Behin, J. & Bahrami, S. 2012 Modeling an industrial dissolved air flotation tank used for separating oil from wastewater. *Chem. Eng. Process. Process Intensif.* **59**, 1–8.

Edzwald, J. K. 2010 Dissolved air flotation and me. *Water Res.* **44** (7), 2077–2106.

Edzwald, J. K., Tobiason, J. E., Amato, T. & Maggi, L. J. 1999 Integrating high rate dissolved air flotation technology into plant design. *J. Am. Water Works Assoc.* **91** (12), 41–53.

Fukushi, K., Tambo, N. & Matsui, Y. 1995 A kinetic model for dissolved air flotation in water and wastewater treatment. *Water Sci. Technol.* **31** (3–4), 37–48.

Haarhoff, J. & Edzwald, J. K. 2001 Modelling of floc-bubble aggregate rise rates in dissolved air flotation. *Water Sci. Technol.* **43** (8), 175–184.

Haarhoff, J. & Edzwald, J. K. 2004 Dissolved air flotation modelling: Insights and shortcomings. *J. Water Supply Res. Technol.-AQUA* **53** (3), 127–150.

Han, M. 2002 Modeling of DAF: The effect of particle and bubble characteristics. *J. Water Supply Res. Technol.-AQUA* **51** (1), 27–34.

Kwak, D.-H. & Kim, M.-S. 2013 Feasibility of carbon dioxide bubbles as a collector in flotation process for water treatment. *J. Water Supply Res. Technol.-AQUA* **62** (1), 52–65.

Lakghomi, B., Lawryshyn, Y. & Hofmann, R. 2012 Importance of flow stratification and bubble aggregation in the separation zone of a dissolved air flotation tank. *Water Res.* **46** (14), 4468–4476.

Leppinen, D. M. & Dalziel, S. B. 2004 Bubble size distribution in dissolved air flotation tank. *J. Water Supply Res. Technol.-AQUA* **53** (8), 531–543.

Leppinen, D. M., Dalziel, S. B. & Linden, P. F. 2001 Modelling the global efficiency of dissolved air flotation. *Water Sci. Technol.* **43** (8), 159–166.

Lundh, M., Jönsson, L. & Dahlquist, J. 2002 The influence of contact zone configuration on the flow structure in a dissolved air flotation pilot plant. *Water Res.* **36** (6), 1585–1595.

Oliveira, C. & Rubio, J. 2012 A short overview of the formation of aerated flocs and their applications in solid/liquid separation by flotation. *Minerals Eng.* **39**, 124–132.

Rubio, J., Carissimi, E. & Rosa, J. J. 2007 Flotation in water and wastewater treatment and reuse: recent trends in Brazil. *Int. J. Environ. Pollut.* **30** (2), 193–207.

Ryu, G. N., Park, S. M., Lee, H. I. & Chung, M. K. 2011 Numerical study of effect of DAF-tank shape on flow pattern in separation zone of dissolved air flotation. *Korean Soc. Mech. Engr-B* **35** (8), 855–860.

Santana, R. C., Ribeiro, J. A., Santos, M. A., Reis, A. S., Ataíde, C. H. & Barrozo, M. A. S. 2012 Flotation of fine apatitic ore using microbubbles. *Sep. Purif. Technol.* **98**, 402–409.

Tambo, N., Matsui, Y. & Fukushi, K. 1986 *A kinetic study of dissolved air flotation*. World Congress of Chemical Engineering, Tokyo, Japan, 200–203.

Wang, L. K., Fahey, E. M. & Wu, Z. 2005 Dissolved air flotation. In: *Physicochemical Treatment Processes. Handbook of Environmental Engineering*, Vol. 3 (L. K. Wang, Y. T. Hung & N. K. Shammas, eds). Humana Press, Totowa, NJ, USA, pp. 431–500.

First received 16 February 2015; accepted in revised form 17 July 2015. Available online 21 August 2015